Analysis of Loading Distribution for SRB and TSRB Combined Bearing

Lei Shi [a,b,*], Jiangang Wang [a,b], Kai Luo [a,b], Ding Feng [a,b,*], Hong Zhang [a,b], Enming Miao[c]

a. School of Mechanical Engineering, Yangtze University, Hubei Jingzhou, 434023, China

b. Hubei Engineering Research Center of Oil and Gas Drilling and Completion Tools, Jingzhou 434023, China

c. Chongqing University of Technology, College of Mechanical Engineering, Chongqing 401135, China

[*]Corresponding Author: Ding Feng. Email: fengd0861@163.com. Tel: +86 13607219921

Co-Corresponding Author: Lei Shi. Email: shilei0909@163.com. Tel: +86 15927864976

Received: XXXX; Accepted: XXXX.

Abstract: Combined bearings are consisted of spherical roller bearings and thrust spherical roller bearings, which are important supports in various low-speed heavy-duty mechanisms and the stability of their running state is a key ensure to supporting the normal operation of the mechanism. Basing on the wellbore trajectory control tool, the loading distribution of combined bearing under pure radial and axial forces is studied theoretically. Two kinds of limit state of rolling elements movement named "Odd press" state and "Even press" state is considered and the Hertzian line elastic contact model is used to deal with the contact between roller and raceway. The calculation results of contact stress and radial displacement are very close to the analysis results, and the accuracy of the analysis results is verified by the radial displacement experiment. The results show that the radial load will lead to the radial displacement of the combined bearing axis, which is about 5.81×10^{-3} mm. The radial displacement can affect the guiding accuracy of the tool to a certain extent. The radial displacement can be reduced by adjusting the structural dimensions of the combined bearing. This research can be used to design SRB and TSRB combined Bearing in actual engineering problem.

Keywords: Combined Bearing; Bearing Washer; Loading Distribution; Numerical Simulation; Finite Element Analysis

Nomenclature

SRB	Spherical roller bearing	F_r	Radial force
TSRB	Thrust spherical roller bearings	φ	Any position angle
δ_r	Radial displacement	α_e	contact angle
$\delta_{r\varphi}$	Normal component of radial displacement	$\delta_{e\varphi}$	Normal displacement of rolling elements
K	Stiffness coefficient	D_w	Equivalent diameter of rolling element
$Q_{e\varphi}$	Normal force of rolling elements	Q_e	The rolling elements' contact force
l	Length of rolling element	Z	The number of the rolling elements
J_{ra}	Radial load distribution coefficients for "odd press"	ε	Coefficient by bearing type
δ_e	Normal contact displacement	δ_a	Axial displacement
K	stiffness coefficient		

1 Introduction

Combined bearing is specially designed and manufactured for different using branches of industry. It can bear

both radial and axial loading. Due to the difference of loading direction, lubrication condition and dustproof requirements, there are many series combination for designers to selection [1]. In order to change the direction of the bit while not affect its rotation, the wellbore trajectory control tool needs the combined bearing to support rotation and deflection of tool spindle.

In the 1970s, combine bearings to meet the demands of high-performance drilling applications were created. Zhuo has developed a high-speed spherical bearing with good results. Halliburton has added a spherical roller bearing to the combination of two thrust spherical roller bearing forms proposed by Japan National Oil Corporation to reduce the impact of bit impacts on the bearing and to enable it to withstand higher temperature and speed requirements.

The combined bearing of wellbore trajectory control tool consists of a spherical roller bearing (SRB) and two thrust spherical roller bearings (TSRB), as shown in Figure 1. The raceway of two TSRB outer ring forms the first sphere of the tool spindle for rotation and deflection. The raceway of SRB outer ring forms the second sphere to correct this rotation and deflection. Under the condition of borehole trajectory control tool deflection, the combined bearing deflects with the tool spindle. The outer ring raceways of the thrust self-aligning roller bearing at both ends form an outer sphere to support the deflection of the spindle, and the outer ring raceways of the central self-aligning roller bearing form an inner sphere to support the deflection of the spindle. The deflection of the tool spindle occurs under the joint support of the inner and outer spheres formed by the combined bearing. In the drilling processes, the working state of the bearing will change with the bending of the spindle. When the stress of the bearing exceeds its endurance, the bearing will fail [2,3]. The study of loading distribution for SRB and TSRB combined bearing in wellbore trajectory control tool is very significant to ensure the correct drilling and the design of combined bearing.

2 The Theory Study of Loading Distribution for SRB and TSRB Combined Bearing

2.1 The force distribution under pure radial loading

Before the study of bearing's radial loading distribution, firstly two kinds of limit state of bearing movement should be taken into an account. In the state Figure 2(a), radial loading action line goes through the center of rolling elements. The number of rolling element which contact with raceway at this time, it can only be an odd number and this state is called the "odd press" state. In the state Figure 2(b), the loading just acts on the bisector of angle between two rolling elements. The number of rolling element which contact with raceway at this time, it can only be an even number and this state is called the "even press" state [4].

According to classical bearing analysis theory, the theory of rigid ring is adopted [5,6]. This assumption greatly simplifies the analysis process, and its calculation results have a certain precision. So, analyzing the combination bearing in wellbore trajectory control tool, the above assumption would be adopted.

As shown in

Figure **4:** Displacement distribution under typical contact

, the inner and outer circle of bearing are assumed that produce relative displacement δ_r under the action of radial force F_r. So the displacement component in any position angle φ is:

$$\delta_\varphi = \delta_r \cos\varphi \tag{1}$$

Before loading to the bearing, certain measures are usually taken to preload the bearing, it can reduce bearing clearance to zero or negative. In this way the bearing stable operation can be ensured. Therefore, when building mathematical models, we can assume that the bearing radial clearance is zero. From Figure 4, the normal component of radial displacement $\delta_{r\varphi}$ is:

$$\delta_{e\varphi} = \delta_{r\varphi} \cos\alpha_e = \delta_r \cos\varphi \cos\alpha_e \tag{2}$$

and from the relation between loading and displacement, the following formula enables to calculate $Q_{e\varphi}$ force:

$$Q_{e\varphi} = K\delta_{e\varphi}^{\ \varepsilon} \tag{3}$$

K is the stiffness coefficient, the value is given by the following formula [7]: $K = 2.89 \times 10^4 l^{0.82} {D_w}^{0.11}$. In this formula, l is the length of rolling element, mm; D_w is the equivalent diameter of rolling element, mm; exponent ε can be selected according to bearing type. As the two types of bearings in this article are roller bearing, the value of ε

is 10/9. From Eq. (2) and Eq. (3), the relation between the normal force of rolling elements $Q_{e\varphi}$ in the position angle φ and the biggest normal force of rolling element Q_e is as follows:

$$Q_{e\varphi} = Q_e(\cos\varphi)^{10/9} \tag{4}$$

So under the condition of the contact, the equilibrium equation can be established as follows:

$$F_r - \sum_{\varphi\geq-\pi/2}^{\varphi\leq\pi/2} Q_{e\varphi}\cos\alpha_e\cos\varphi = 0 \tag{5}$$

The above equation only consider the loading situation when φ ranges from $-\frac{\pi}{2}$ to $\frac{\pi}{2}$, as $\delta_{r\varphi} \leq 0$ when φ is in other scope.

When assuming the number of the rolling elements is Z, the equilibrium equation under "odd press" state is as follows:

$$F_r = \sum_{\varphi\geq-\pi/2}^{\varphi\leq\pi/2} Q_{e\varphi}\cos\alpha_e\cos\varphi = Q_e Z J_{ra}\cos\alpha_e \tag{6}$$

Therefore, the following equation can be obtained:

$$Q_e = \frac{F_r}{ZJ_{ra}\cos\alpha_e} \tag{7}$$

where, J_{ra} is the radial loading distribution coefficient under "odd press" state, its value is:

$$J_{\mathrm{ra}} = \frac{1}{Z}\left\{1+2\sum_{\varphi=2\pi/Z}^{\varphi\leq\pi/2}(\cos\varphi)^{19/9}\right\} \tag{8}$$

The equilibrium equation under "even press" state is as follows:

$$F_r = \sum_{\varphi\geq-\pi/2}^{\varphi\leq\pi/2} Q_{e\varphi}\cos\varphi = Q_e Z J_{rb}\cos\alpha_e \tag{9}$$

Therefore

$$Q_e = \frac{F_r}{ZJ_{rb}\cos\alpha_e} \tag{10}$$

In "even press" state, Q_{e} doesn't exist, and the actual maximum loading appears in a pair of rolling elements which is the closest distance to the load line. Its value is:

$$Q_e' = Q_e\left[\cos\left(\frac{\pi}{z}\right)\right]^{10/9} \tag{11}$$

2.2 The force distribution under pure axial loading

Under the action of pure axial loading, inner and outer circle of bearing will produce a relative displacement δ_{a}, which is as shown in Figure 5. Now the contact loading and displacement of the rolling elements are the same. As the outer ring is fixed, the rolling elements and the outer ring will generate contact displacement under the action of axial displacement. The rolling elements' contact force is Q_{e}. The normal contact displacement is δ_e, and the contact angle is α_{e}.

As the normal contact displacement which caused by axial force is:

$$\delta_e = \delta_a\sin\alpha_e \tag{12}$$

Therefore, the contact loading of rolling element can be obtained as follows:

$$Q_e = K\delta_e^{10/9} = K\delta_a^{10/9}\left(\sin\alpha_e\right)^{10/9} \tag{13}$$

So the axial direction's component of the contact loading is:

$$Q_{ea} = Q_e\sin\alpha_e = K\delta_a^{10/9}\left(\sin\alpha_e\right)^{10/9}\sin\alpha_e = K\delta_a^{10/9}\left(\sin\alpha_e\right)^{19/9} \tag{14}$$

When the number of bearing's rolling element is Z, the equilibrium equation is:

$$F_a - ZK\delta_a^{10/9}\left(\sin\alpha_e\right)^{19/9} = 0 \cdot \tag{15}$$

So axial displacement is obtained as follows:

$$\delta_a = \left(\frac{F_a}{ZK\left(\sin\alpha_e\right)^{19/9}}\right)^{9/10} \tag{16}$$

2.3 Structural parameters, loads and calculation results

(1) Combined bearing structural parameters and loads

As shown in Table 1, Combined bearing structural parameters is used to calculate the stiffness coefficient. In the condition of steering drilling, the radial force that transfers to combination bearing is 12733N and axial force is 1089N, which is from the earlier research on wellbore trajectory control tool[8].

(2) Calculation results

Using the formulas in 2.1 and 2.2, we can calculate the contact load for each bearing, as shown in Table 2 and Table 3: Load distribution of TSRB.

By using the classical Hertz elastic contact theory, the maximum contact stress between roller and raceway is about 312.1MPa and radial displacement is about 2.7×10^{-3}mm.

3 The Finite Element Analysis (FEA) of SRB and TSRB Combined Bearing

There are two kinds of working state when wellbore trajectory control tool is under typical working condition, that is, the normal drilling and steering drilling. In normal drilling, spindle only sustains the axial bit pressure, and it will not bend. In steering drilling, on one hand, the spindle sustains the axial bit pressure. On the other hand, it also sustains the radial force which is applied by eccentric mechanism, and this radial force leads the spindle bending. So during the FEA of SRB and TSRB Combined Bearing, two cases will be divided.

3.1 Modeling, material selection and meshing of combined bearing

Due to the complexity of combination bearing structure and lots of contact area, it would not only consume time but also not easy to modify using the finite element software. In order to improve the efficiency of modeling, the Solidworks software is used to establish the three-dimensional model of bearing [9,10]. So, we use the multi-physics field analysis software COMSOL for analyzing combined bearing's load situation in two kinds of working conditions. So, this working condition is typical drilling and steering drilling.

In the operation of wellbore trajectory control tool, relatively high-speed rotation and vibration will generate. Rolling elements must withstand repeated alternating stress on one hand, on the other hand there is relative slip between rolling elements and race. So, we demand rolling elements having good mechanical property. For this reason, bearing steel is selected as the material of this bearing [11,12].

The manner of free mesh is adopted meshing combination bearing's grid. For the contact area, we can use the manner of local refinement to ensure the accuracy of calculation.

3.2 Adding boundary conditions

Because the radial, tangential and axial freedom of bearing race which contact with the shell are limited, the three bearing race need to be added fixed constraint. In addition, the spindle only sustains the axial bit pressure under normal working condition. At this time, the combination bearing only sustains the pre-tightening force. Therefore, under typical working condition, the race of two thrust spherical roller bearing need to be added axial force of 1089 N.

In the condition of steering drilling, the spindle not only sustains the bit pressure but also generate bending. Through the mechanical analysis of the spindle [13,14], we can know that the eccentric ring needs to be added radial force of 16918 N, when the spindle generates maximum deflection. But the radial force that transfers to combination bearing is 12733 N. Therefore, when conducting boundary loading, the shaft circle of spherical roller bearing and the inside of two gaskets need to be added radial force of 12733 N. At the same time, the both ends of thrust spherical roller bearing should also be added the pre-stressing force of 1089 N.

All the data above such as axial force(1089N) and radial force(12733 N) are from the earlier research on wellbore trajectory control tool which was supported by the national natural science foundation of China（51275057）.

3.3 Results and analysis

(1) The results and analysis of normal drilling

For the response of bearing under simulation of loading, the attention was focus on the rolling element behavior. Through the above pre-treatment and solving, we can get the stress and displacement diagram of combination bearing during typical drilling. They are shown in Figs. 6,7.

From the stress and displacement distributions, we can see the effect of pre-stressing force. The maximum stress is on the thrust spherical roller bearing. Reaching the value of 2.94 MPa. In addition, the displacement of the thrust spherical roller bearing inside race is most obvious. The largest displacement is 5.85×10^{-5}mm.

From the pictures, we can see the loading is creates by all rolling elements evenly under the effect of axial pre-tightening force. This is consistent with the theoretical study result in 2.2 under pure axial loading and the stress mainly concentrated in the contact area between rolling element and raceway.

(2) The results and analysis of steering drilling

Under steering drilling conditions, the stress and displacement distributions in combined bearing are shown in Fig. 8~11.

From the stress and displacement distribution of combined bearing, we can see this produces large stress and displacement on the radial load line of the rolling element and raceway contact parts, when the outer ring is fixed. The stress value away from the area will gradually decrease. There, the maximum stress value is 345 MPa, and the biggest displacement is 1.78×10^{-3} mm.

From the analysis, the loading response of bearing is mainly concentrated on the contact area of rolling element and raceway. And under the action of radial force, the upper circle rolling element carrying is larger, while the under circle rolling element is almost not affected by the loading. In addition, we can see rolling element loading distribution has the characteristics of “be big in the middle and small at both ends". The radial force and axial force are 12733 N and 1089 N respectively when steering drilling. Now the influence of the axial force to the rolling element loading response is very small, the action of pure radial load can be thought to be condition of steering drilling. So this is consistent with the theoretical study result in 2.1 under pure radial loading.

Fig. 10 and Fig. 11 are the stress and displacement distribution of the section that cross the axis and the radial loading action line of the combined bearing. From the figure, the loading that spherical roller bearing sustains is larger than the thrust spherical roller bearing. The stress mainly concentrates on the contact between the rolling element and raceway. In addition, under the action of radial loading, the gasket will generate an axial compression to the thrust spherical roller bearing on both sides. This compression will compel the thrust spherical roller to produce secondary stress. Therefore, in order to reduce the stress concentration of bearing, the bearing washer should be conducted reasonable design.

(3) The results comparative of experimental, computational and finite element methods

The contact stress between roller and raceway is difficult to be measured by experiment under actual working conditions. The experiment method and experimental results of the wellbore trajectory control tool have been described in reference 3. The calculation results, simulation results and experimental results are summarized, as shown in Table 4.

The comparison between the experimental results and calculation results as well as simulation results shows that the radial displacement results obtained by the three methods are very close to each other. The experimental results higher than the analysis results are caused by tool weight and uncontrollable factors such as machining error.

4 Conclusion

In this paper, combined with SRB and TSRB combined bearing of wellbore trajectory control tool, the formula of the bearing’s loading distribution is derived. The three-dimensional model of combined bearing is established using Solidworks software. The loading situation of combined bearing is analyzed by the COMSOL software. Through the comparison of theoretical study results and FEA results, the following conclusions can be obtain:

(1)When the combined bearing sustains pure axial force, the loading response is evenly taken by the rolling element. And the most of the pre-tightening force is sustained by thrust spherical roller bearing, while the spherical roller bearing is almost not affected by loading. Therefore the mechanical properties of thrust spherical roller bearing should be superior to that of the spherical roller bearing.

(2) When the SRB and TSRB combined bearing sustains pure radial force, the loading response of rolling element is the largest through the action line which is in the centre of the bearing. The loading on both sides of bearing is

reduced in turn, and the stress is mainly concentrated in the contact part between the rolling elements and raceway. So the mechanical behavior of rolling elements and raceway should be taken into consideration seriously in the structure design of combination bearing.

(3) The secondary stress on both sides of the bearing is generated by the radial load of the bearing washer. In order to reduce the stress concentration of bearing, the structure of the bearing washer needs reasonably designed to prolong the service life of bearing in the next step.

Acknowledgement: This work of the paper was supported by the scientific research program of Hubei education department(Q20181315)and Hubei Technology Innovation Project (major project) (2019AAA010). as well as Yangtze University Excellent Master Degree Thesis Cultivation Program (YS2018023).

Conflicts of Interest: The authors declare that they have no conflicts of interest to report regarding the present study.

References

1. Huang, L.L., Xue, Q.L., Liu, B.L., et al. “Dynamic Reliability Analysis of Rotary Steering Drilling System”, *Mechanical Sciences*, 10(1),79-90 (2019).

2. Feng, D., Lu, C., Zhang, H., et al. “Research on Control of Steering Movement of Well Trajectory Control Tool”, *Journal of Oil Field Equipment*,46,6-10 (2017).

3. Zhang, H., Feng, D., Wei, S.Z., et al. “A New Predicting Method of Build-up Rate of Steering Tools Based on Kriging Surrogate Model”, *Arabian Journal for Science and Engineering*, 43(9): 4949-4956 (2018).

4. Huang, H.J., Wang, X., Xue, K.J. “Effect of Cage Wear in Rolling Bearing on Bearing Failure”, *Journal of Lubrication Engineering*,46(07),128-136 (2021).

5. Wang, Y., Tse, P.W., Tang, B.P., et al. “Order spectrogram visualization for rolling bearing fault detection under speed variation conditions”, *Mechanical Systems and Signal Processing*, 122,580-596 (2018).

6. Vashisht R.K., and Peng, Q.J. “Crack detection in the rotor ball bearing system using switching control strategy and Short Time Fourier Transform”, *Journal of Sound and Vibration*, 432,502-529 (2018).

7. Harris, O.O., and Osisanya, S.O. “Evaluation of equivalent circulating density if drilling fluids under high-pressure/high-temperature conditions”, *SPE*: 97018 (2015).

8. Shi, L., Wang, K.Q., Feng, D., et al. “Wellbore trajectory control tool seal system leakage analysis based on steady gap flow”, *Advances in Mechanical Engineering*, 12, 6(2020).

9. Dong, Y.X., Si, D.H., and Liu, W.S. “Research on parametric design of high-speed spindle”, *Journal of Mining & Processing Equipmen*, 47(02),47-52 (2019).

10. Ma, S.J., Yan, K., Zhang, X.H., et al. “An Accurate Modeling Method and Secondary Development of Bearing Contact-Motion”, *Journal of Xi'an Jiaotong University*, 55(08),33-41 (2021).

11. Bombač, D., Terčelj, M., Peruš, et al. “The progress of degradation on the bearing surfaces of nitrided dies for aluminium hot extrusion with two different relative lengths of bearing surface”, *Wear*, 307,1-2 (2014).

12. S. M. Muzakkir, K. P. Lijesh, Harish Hirani. “Tribological failure analysis of a heavily-loaded slow speed hybrid journal bearing”, *Engineering Failure Analysis*, 40,12-24 (2014).

13. Feng, D., Lv, J.H., Xiang, Z.X., et al. “Failure analysis an optimization of cantilever bearing of borehole trajectory control devices”, *Journal of Science Technology and Engineering*, 16,179-182 (2016).

14. Zhang, H., Xiang, Z.X., Qian, L.Q., et al. “The correlation between the spindle load and the deflecting capacity of the wellbore trajectory control tool”, *Journal of Mechanics in Engineering*, 39,152-157 (2017).

Figure 1: Combined bearing structure diagram

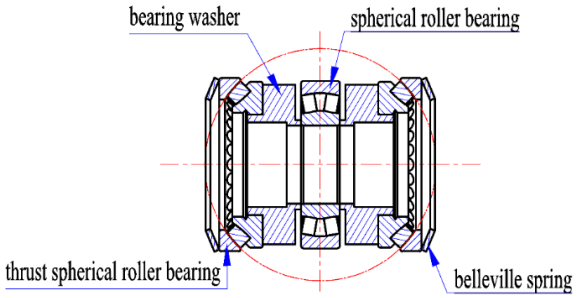

Figure 2: Two kinds of limit state of rolling elements movement

(a) "Odd press" state (b) "Even press" state

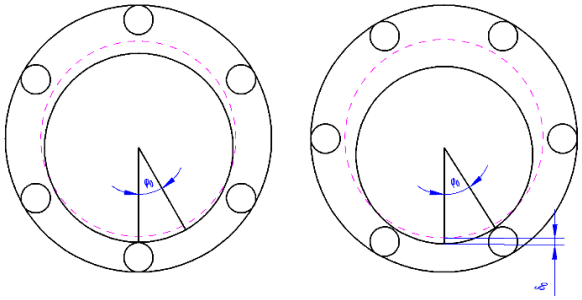

Figure 3: The radial displacement of component

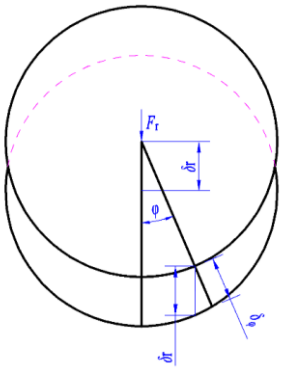

Figure 4: Displacement distribution under typical contact

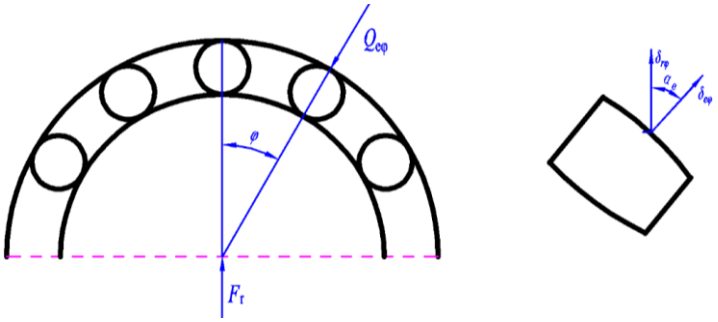

Figure 5: Distribution of loading

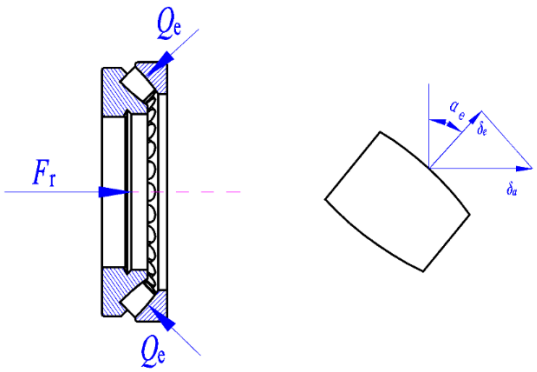

Figure 6: Von Mises stress distribution (unit Pa)

Figure 7: Displacement distribution (unit m)

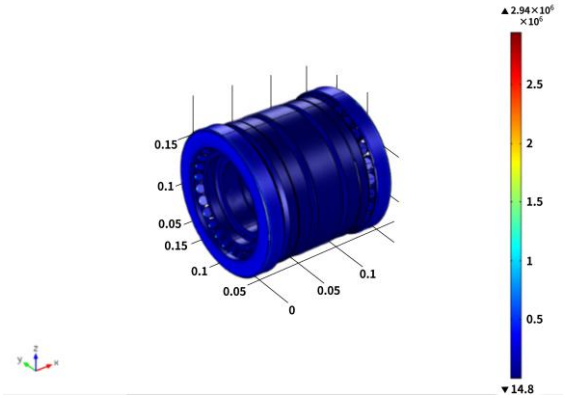

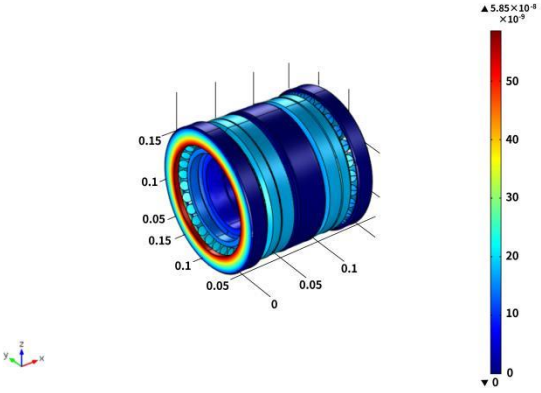

Figure 8: Steering drilling stress (unit Pa)

Figure 9: Steering drilling displacement (unit m)

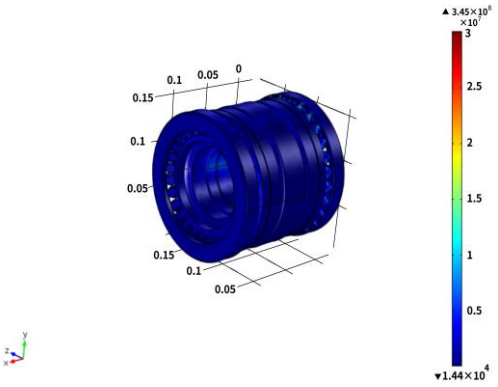

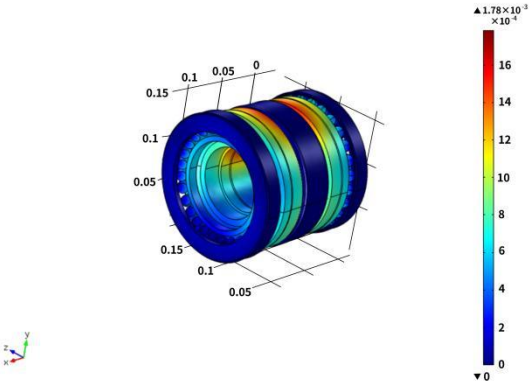

Figure 10: Stress of XY plane (unit Pa)

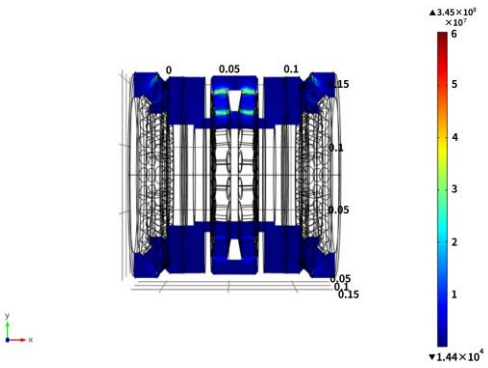

Figure 11: Displacement of XY plane (unit m)

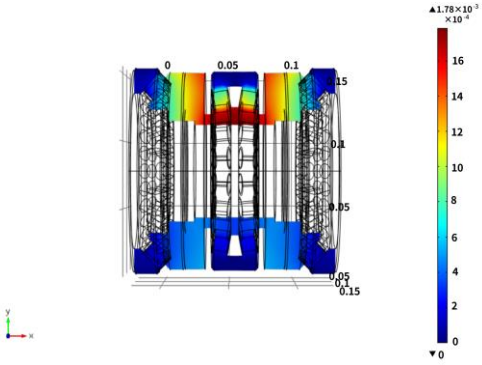

Table 1: Wellbore trajectory control tool combined bearing structural parameters

Name of parameter	Parameter value	Unit
SRB bearing contact angle α_e	10.2	°
SRB bearing outer diameter D_{mo}	155	mm
SRB bearing inner diameter D_{mi}	70	mm
number of rollers for SRB bearing Z_m	18	/
TSRB bearing contact angle α_t	45	°
TSRB bearing outer diameter D_{to}	155	mm
TSRB bearing inner diameter D_{ti}	70	mm
number of rollers for TSRB bearing Z_t	21	/
length of rolling element l	11.67	mm
equivalent diameter of rolling element D_w	16.30	mm

Table 2: Load distribution of SRB

φ (°)	0	±20	±40	±60	±80
Q_φ (N)	2938.00	2741.80	2184.97	1360.11	419.99

Table 3: Load distribution of TSRB

φ (°)	0	±12.86	±25.71	±38.57	±51.43	±64.29	±77.14
Q_φ (N)	2627.02	2553.93	2339.59	1998.48	1554.16	1038.83	494.67

Table 4: The results summary for combined bearing

The result type	Contact stress	Radial displacement
calculation results	312.1 MPa	2.7×10^{-3} mm
simulation results	345 MPa	1.78×10^{-3} mm
experimental results	—	$5.81\text{-}5.95\times10^{-3}$ mm

Biographies

Lei Shi received his Ph.D. in Engineering from Changjiang University in 2017, his major in oil field equipment, published several papers and participated in the translation of a series of books on foreign oil and gas exploration and development progress. He has participated in 6 projects at national and provincial levels published 8 first-author academic papers in relevant academic journals.

Jiangang Wang is a current Ph.D. student at Yangtze University and received his Master's degree at Yangtze University in 2021. As a major participant, he has participated in 3 national provincial and ministerial projects and Published 4 related papers. His research interests: theoretical and technical application research in the design, diagnosis and dynamic simulation of petroleum machinery.

Ding Feng is a Professor of Mechanical Engineering at Yangtze University, China. He received his Ph.D. at the China University of Petroleum (Beijing). His main research areas are design, testing and diagnostics of oil and gas drilling and completion tools and equipment and offshore engineering equipment and tubular column mechanics and dynamic simulation technology. He has participated in nearly 90 projects at national and provincial levels and published 179 relevant academic papers.

Kai Luo was admitted to the School of Mechanical Engineering, Yangtze University for his master's degree in September 2019. As the participants involved in the two national natural science foundation of China, is mainly responsible for structure simulation and test related job. His research direction is mechanical system simulation and diagnosis technology.

Hong Zhang, PhD, Associate Professor, Master's Supervisor. Director of Hubei Mechanical and Electrical Engineering Society. She has presided over 6 vertical projects of provincial and ministerial level sources, such as sub-projects of major special projects of MIIT, Hubei Provincial Department of Education, State Key Laboratory and Hubei Provincial Key Laboratory, etc. She has published more than 20 papers and more than 20 patents. Her research interests are in petroleum equipment research and development.

Enming Miao is a professor and Ph.D. supervisor in the School of Instrument Science and Optoelectronic Engineering at the Hefei University of Technology. His main research interests are precision mechanical engineering, accuracy theory, thermal error compensation of CNC machine tools, and structural design theory and application technology of mechanical thermal robustness. Published more than 50 papers.